Electronic Supplementary Material (ESI) for Physical Chemistry Chemical Physics.
This journal is © the Owner Societies 2022

Supporting Information for On the determination of Lennard-Jones parameters for polyatomic molecules

Huangrui Mo[a,b,c], Xiaoqing You[a,b,*], Kai Hong Luo[d], Struan H Robertson[e]

[a] *Center for Combustion Energy, Tsinghua University, Beijing 100084, China*
[b] *Key Laboratory for Thermal Science and Power Engineering of the Ministry of Education, Tsinghua University, Beijing 100084, China*
[c] *State Key Laboratory of High Temperature Gas Dynamics, Institute of Mechanics, Chinese Academy of Sciences, Beijing 100190, China*
[d] *Department of Mechanical Engineering, University College London, Torrington Place, London WC1E 7JE, U.K.*
[e] *Dassault Systèmes, BIOVIA, 334, Cambridge Science Park, Cambridge CB4 0WN, U.K.*

List of Figures

*Corresponding author
Email address: xiaoqing.you@tsinghua.edu.cn (Xiaoqing You)

List of Tables

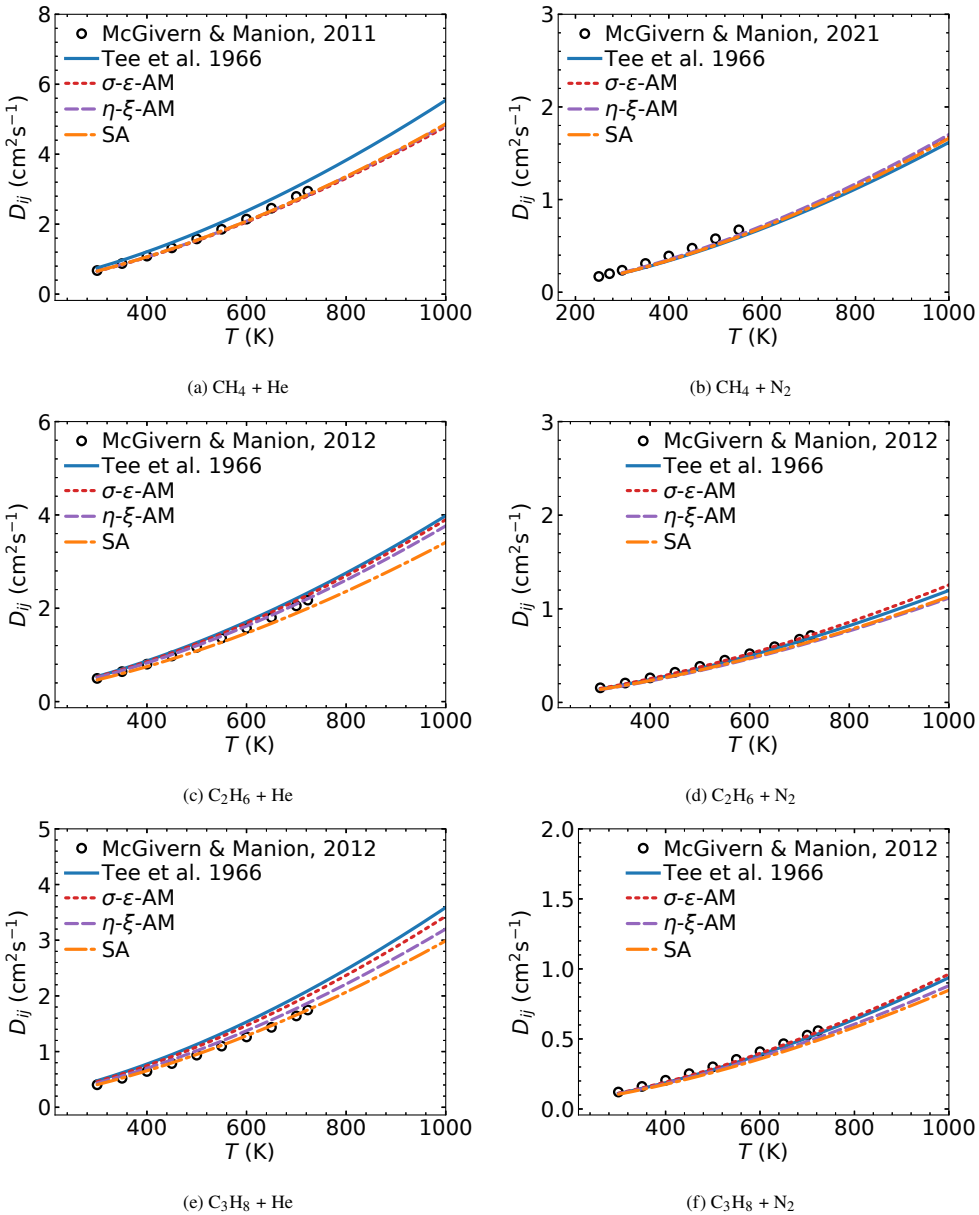

(a) CH_4 + He

(b) CH_4 + N_2

(c) C_2H_6 + He

(d) C_2H_6 + N_2

(e) C_3H_8 + He

(f) C_3H_8 + N_2

Figure S-1: Comparison of binary diffusion coefficients of CH_4, C_2H_6, and C_3H_8 in He or N_2. Symbols are experimental diffusion data; solid lines are calculated by empirical parameters; dashed lines are calculated by Lennard-Jones parameters obtained via different averaging rules.

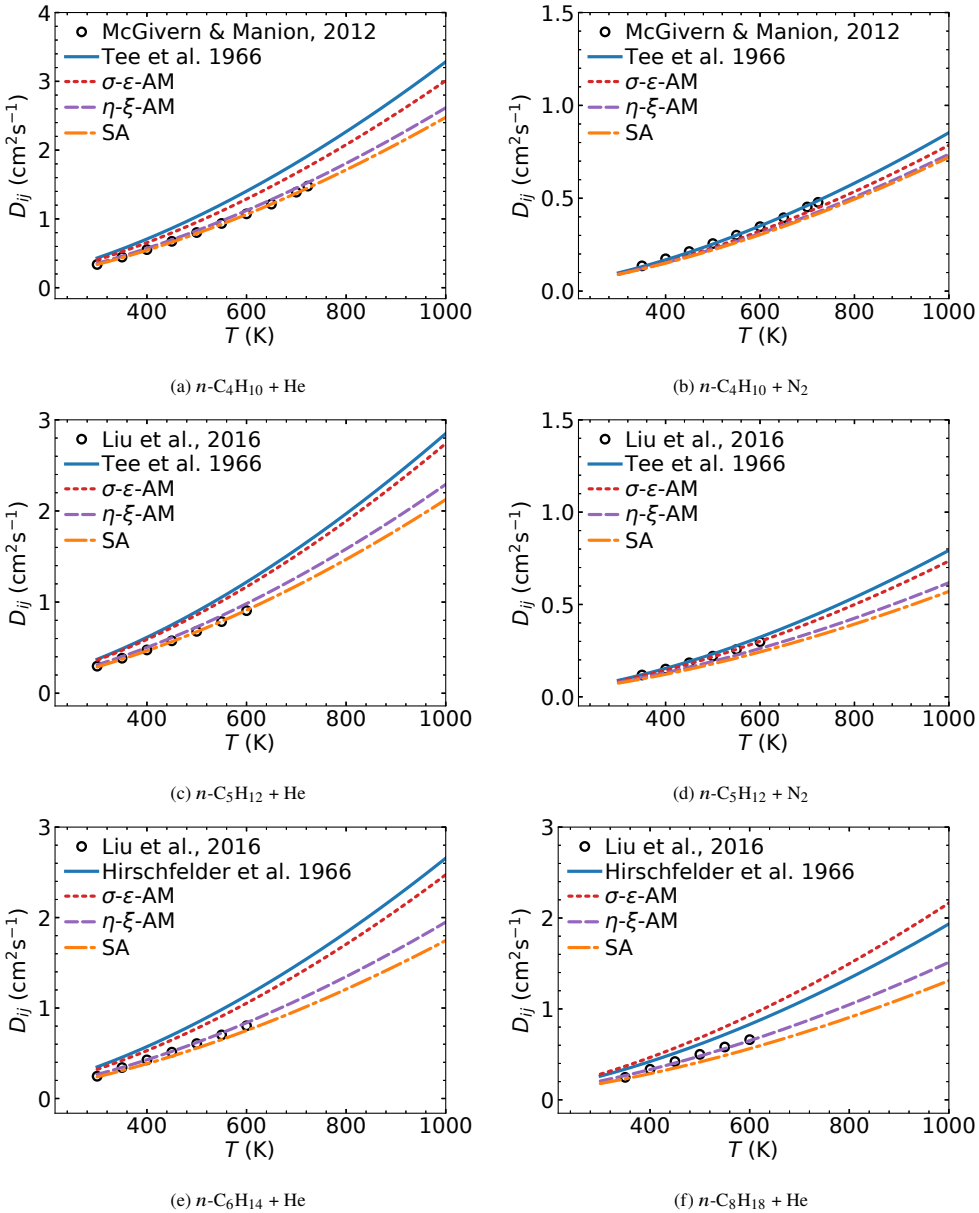

(a) n-C_4H_{10} + He

(b) n-C_4H_{10} + N_2

(c) n-C_5H_{12} + He

(d) n-C_5H_{12} + N_2

(e) n-C_6H_{14} + He

(f) n-C_8H_{18} + He

Figure S-2: Comparison of binary diffusion coefficients of n-C_4H_{10}, n-C_5H_{12}, n-C_6H_{14}, and n-C_8H_{18} in He or N_2.

Table S-1: Parameters for the exp-6 interatomic potential obtained from Jasper and Miller [1].

Bath gas	Atom-atom pair	E_{ij}(Hartree)	B_{ij}(Å)	C_{ij}(Hartree$^{1/6}$ · Å)	D_{ij}(Å)
He	C – He	11.8489	0.2884	0.7941	0.0000
	H – He	6.2486	0.2522	0.5807	0.0000
Ar	C – Ar	153.9332	0.2772	0.9101	0.0000
	H – Ar	18.2093	0.2954	0.9174	0.0000
N_2	C – N	63.6961	0.2861	0.0037	6.0573
	H – N	15.3831	0.2759	0.8316	0.9430
O_2	C – O	170.5952	0.2455	0.8914	2.6329
	H – O	5.0187	0.2887	0.7718	2.6329

[1] A. W. Jasper and J. A. Miller, "Theoretical unimolecular kinetics for CH4 + M <-> CH3 + H + M in eight baths, M = He, Ne, Ar, Kr, H2, N2, CO, and CH4," J. Phys. Chem. A 115, 6438–6455 (2011).

Table S-2: Lennard-Jones parameters for M + M, M = He, Ar, N_2, O_2 obtained from Jasper and Miller [2].

	He	Ar	N_2	O_2
σ (Å)	2.58	3.33	3.68	3.46
ε (K)	10.2	136.5	97.7	107.4

[2] A. W. Jasper and J. A. Miller, "Lennard–Jones parameters for combustion and chemical kinetics modeling from full-dimensional intermolecular potentials," Combust. Flame 161, 101–110 (2014).

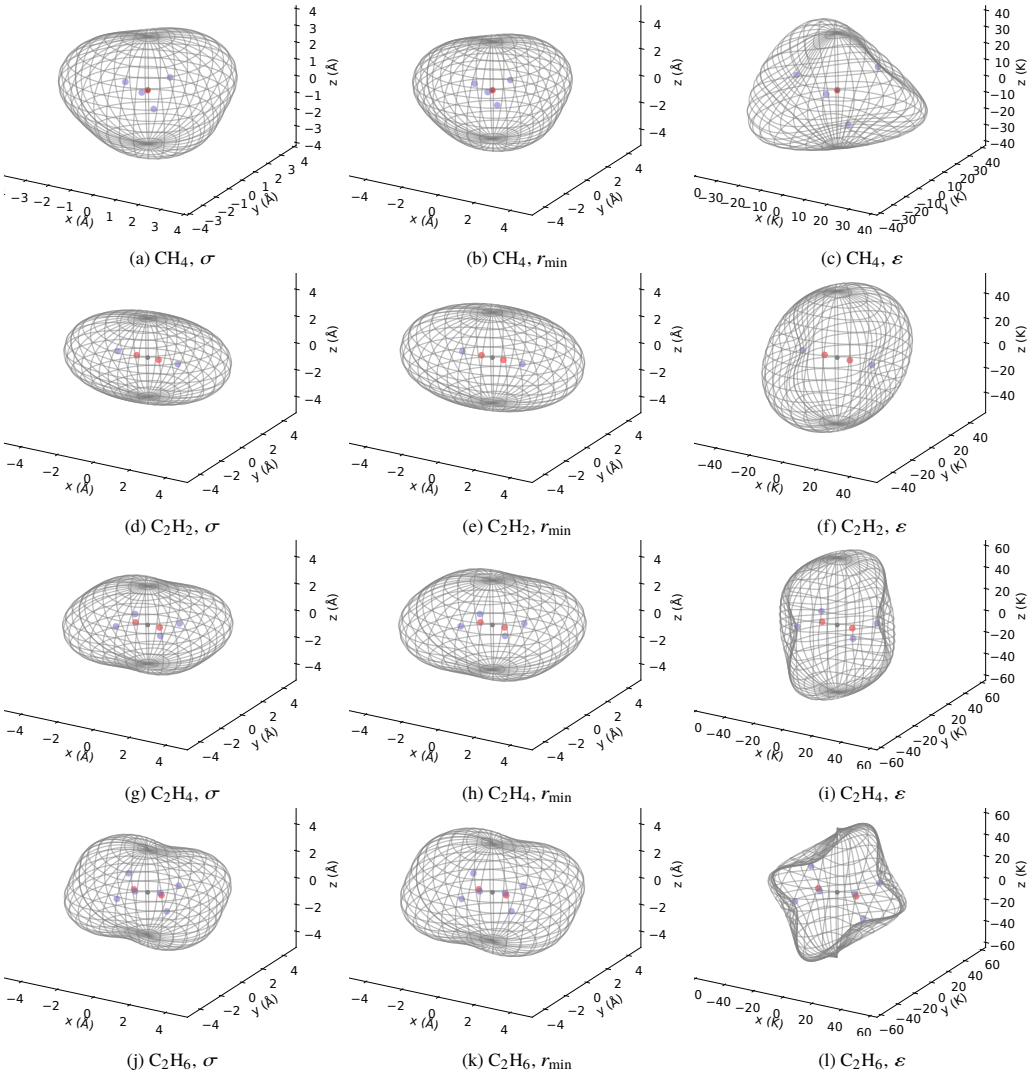

(a) CH_4, σ (b) CH_4, r_{min} (c) CH_4, ε

(d) C_2H_2, σ (e) C_2H_2, r_{min} (f) C_2H_2, ε

(g) C_2H_4, σ (h) C_2H_4, r_{min} (i) C_2H_4, ε

(j) C_2H_6, σ (k) C_2H_6, r_{min} (l) C_2H_6, ε

Figure S-3: Three-dimensional parametric surfaces of the collision diameter σ, well location r_{min}, and well depth ε by the developed iterative search method for a set of target-He pairs.

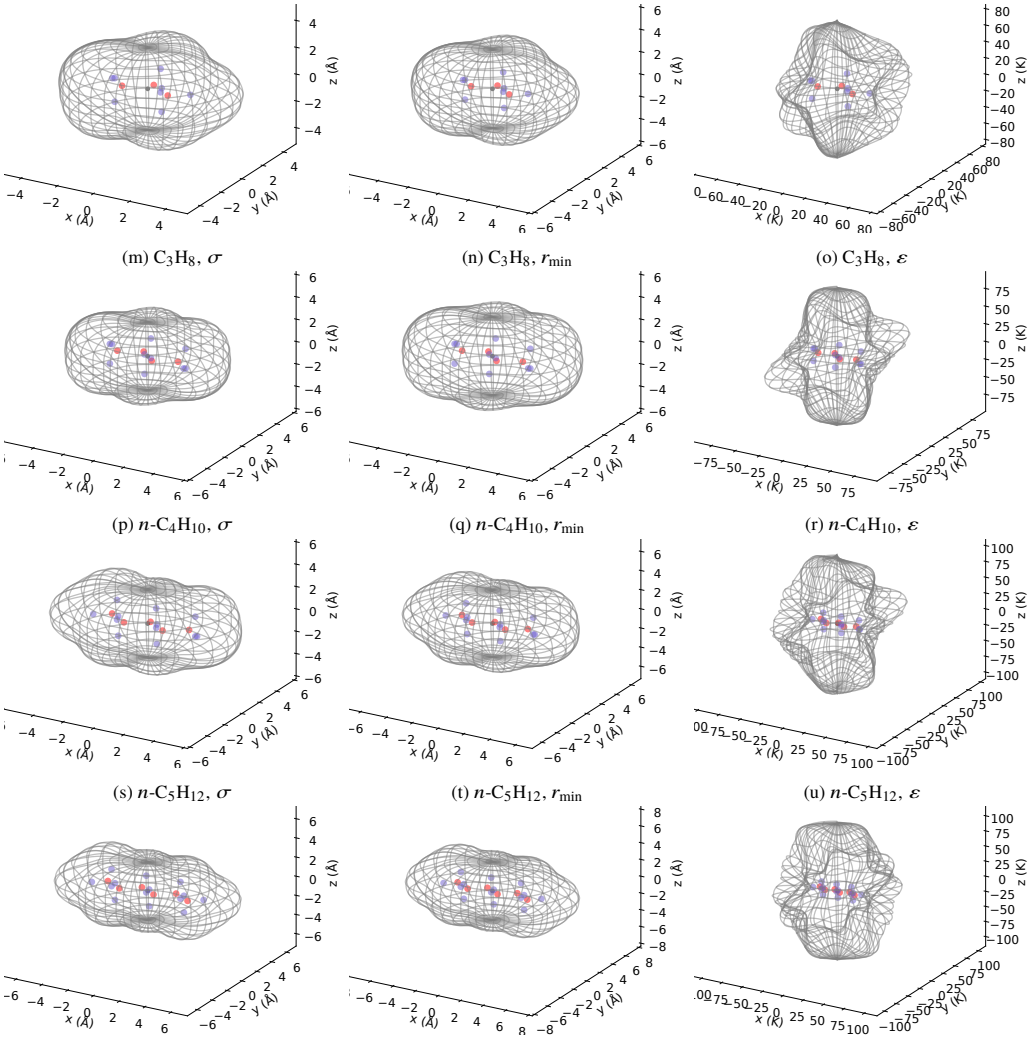

(m) C_3H_8, σ (n) C_3H_8, $r_{\min}$ (o) C_3H_8, ε

(p) n-C_4H_{10}, σ (q) n-C_4H_{10}, $r_{\min}$ (r) n-C_4H_{10}, ε

(s) n-C_5H_{12}, σ (t) n-C_5H_{12}, $r_{\min}$ (u) n-C_5H_{12}, ε

(v) n-C_6H_{14}, σ (w) n-C_6H_{14}, $r_{\min}$ (x) n-C_6H_{14}, ε

Figure S-3: Target-He pairs (continued).

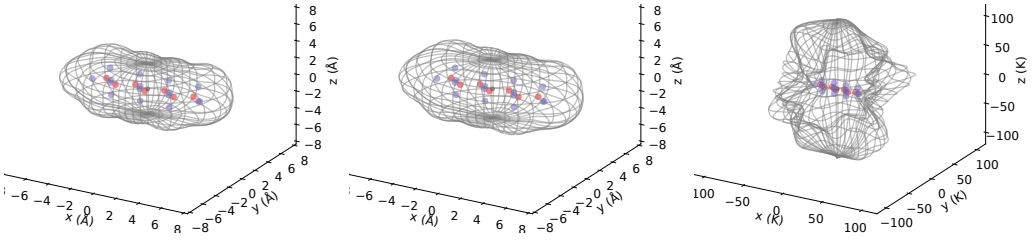

(y) n-C_7H_{16}, σ (z) n-C_7H_{16}, $r_{\min}$ (aa) n-C_7H_{16}, ε

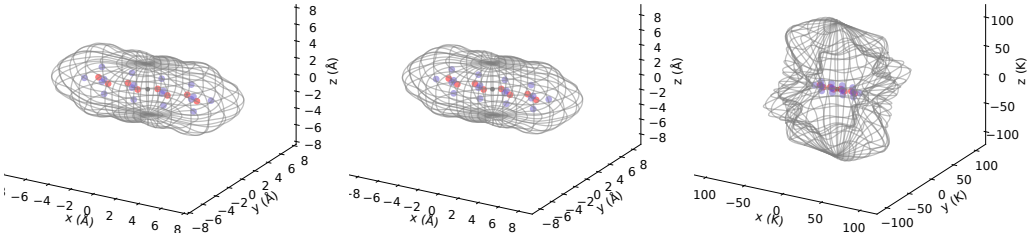

(ab) n-C_8H_{18}, σ (ac) n-C_8H_{18}, $r_{\min}$ (ad) n-C_8H_{18}, ε

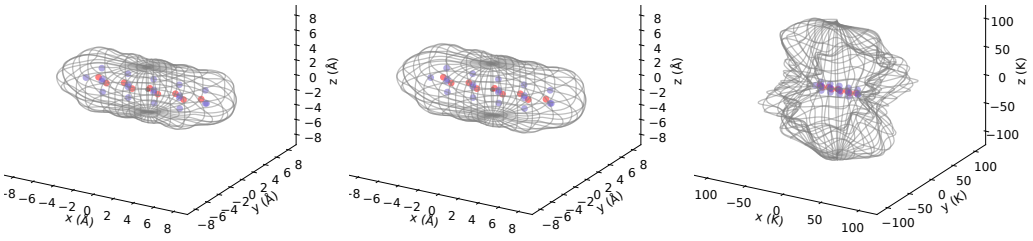

(ae) n-C_9H_{20}, σ (af) n-C_9H_{20}, $r_{\min}$ (ag) n-C_9H_{20}, ε

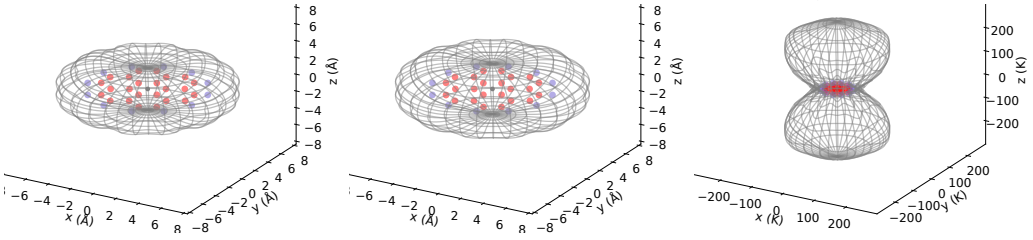

(ah) $C_{24}H_{12}$, σ (ai) $C_{24}H_{12}$, $r_{\min}$ (aj) $C_{24}H_{12}$, ε

Figure S-3: Target-He pairs (continued).

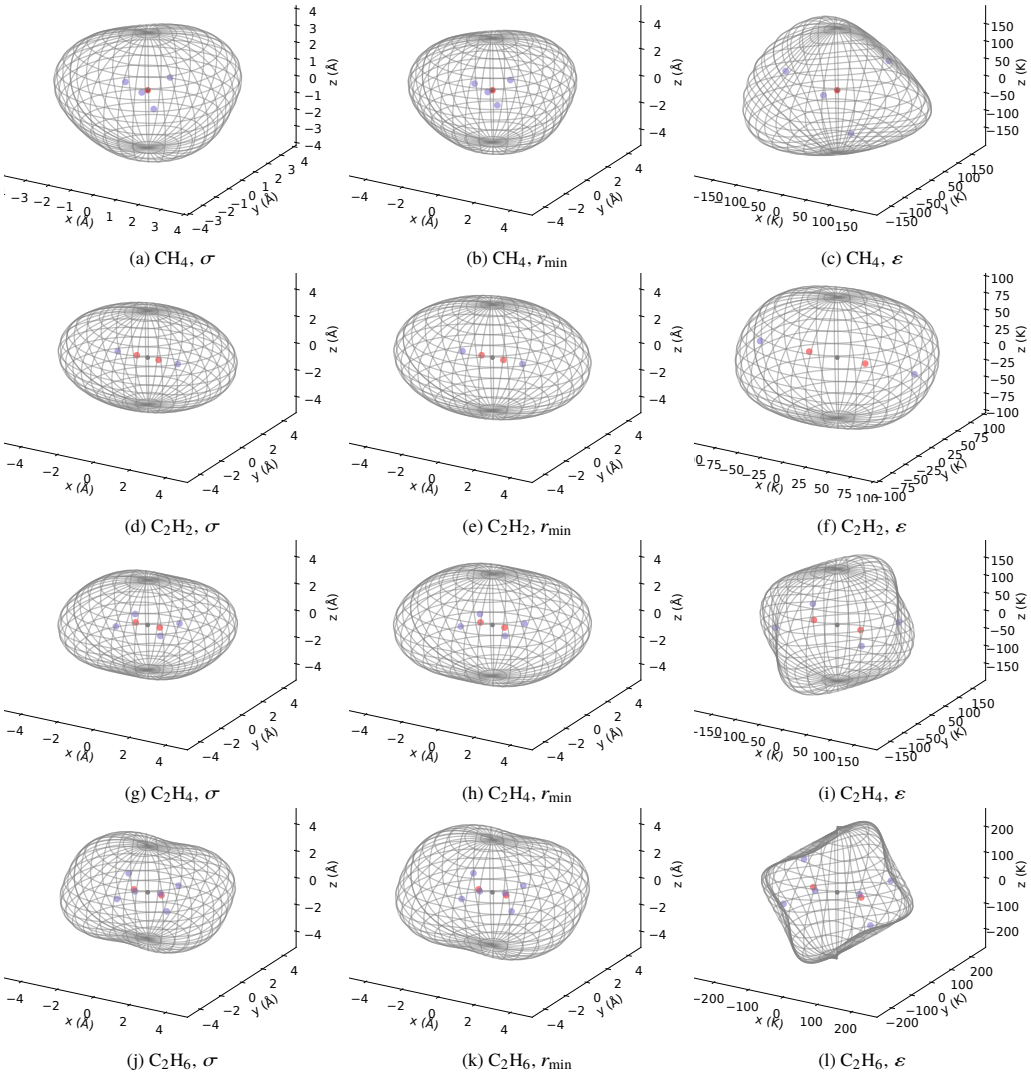

(a) CH_4, σ (b) CH_4, r_{min} (c) CH_4, ε

(d) C_2H_2, σ (e) C_2H_2, r_{min} (f) C_2H_2, ε

(g) C_2H_4, σ (h) C_2H_4, r_{min} (i) C_2H_4, ε

(j) C_2H_6, σ (k) C_2H_6, r_{min} (l) C_2H_6, ε

Figure S-4: Three-dimensional parametric surfaces of the collision diameter σ, well location r_{min}, and well depth ε by the developed iterative search method for a set of target-Ar pairs.

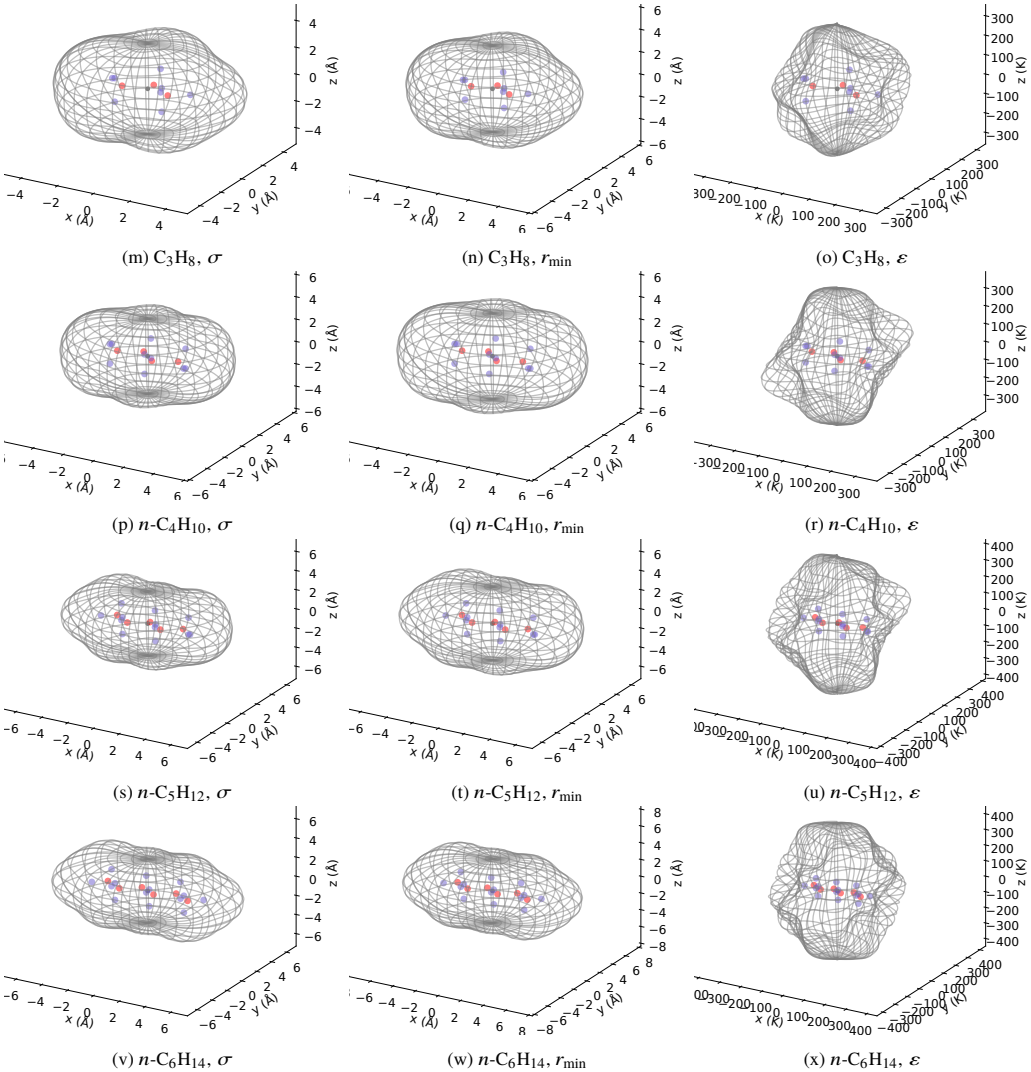

(m) C_3H_8, σ (n) C_3H_8, $r_{\min}$ (o) C_3H_8, ε

(p) n-C_4H_{10}, σ (q) n-C_4H_{10}, $r_{\min}$ (r) n-C_4H_{10}, ε

(s) n-C_5H_{12}, σ (t) n-C_5H_{12}, $r_{\min}$ (u) n-C_5H_{12}, ε

(v) n-C_6H_{14}, σ (w) n-C_6H_{14}, $r_{\min}$ (x) n-C_6H_{14}, ε

Figure S-4: Target-Ar pairs (continued).

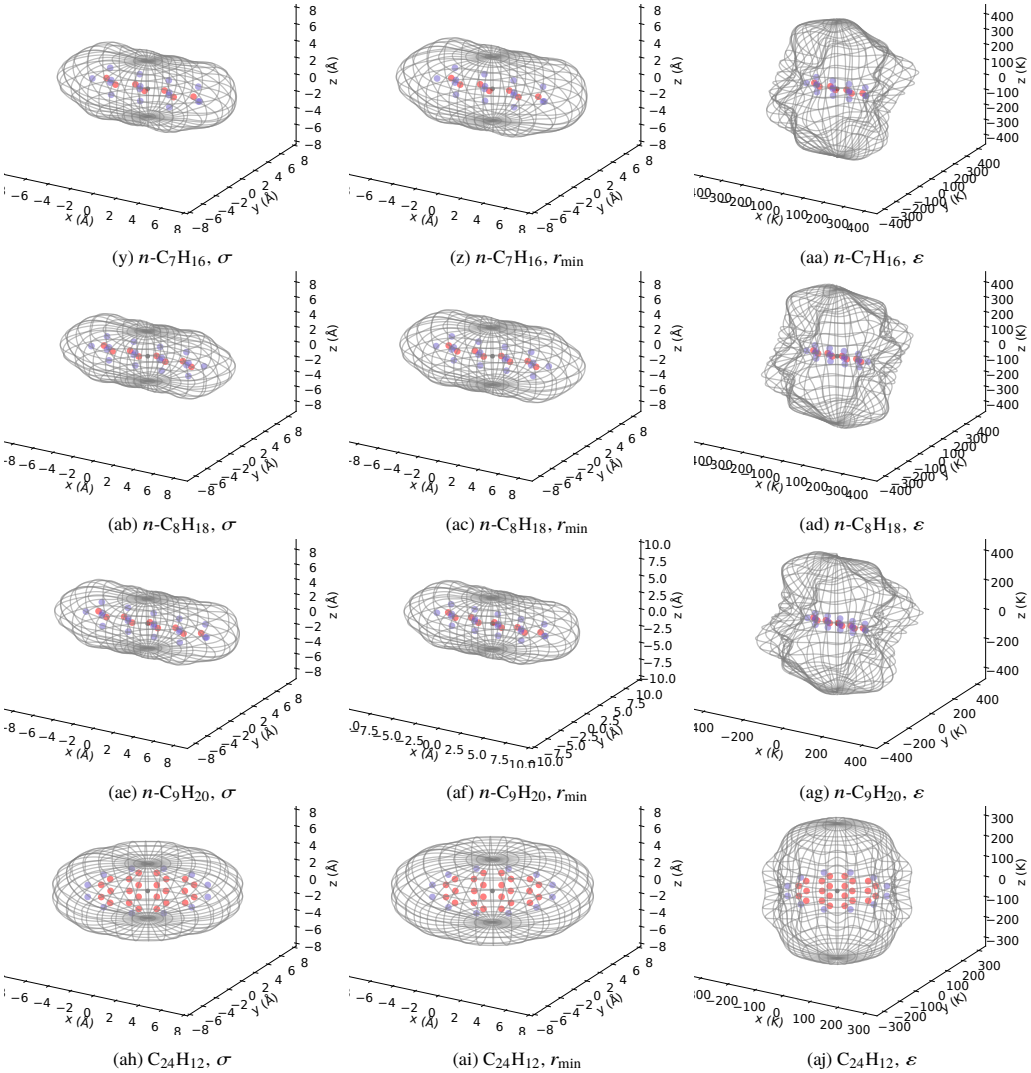

(y) n-C_7H_{16}, σ (z) n-C_7H_{16}, $r_{\min}$ (aa) n-C_7H_{16}, ε

(ab) n-C_8H_{18}, σ (ac) n-C_8H_{18}, $r_{\min}$ (ad) n-C_8H_{18}, ε

(ae) n-C_9H_{20}, σ (af) n-C_9H_{20}, $r_{\min}$ (ag) n-C_9H_{20}, ε

(ah) $C_{24}H_{12}$, σ (ai) $C_{24}H_{12}$, $r_{\min}$ (aj) $C_{24}H_{12}$, ε

Figure S-4: Target-Ar pairs (continued).

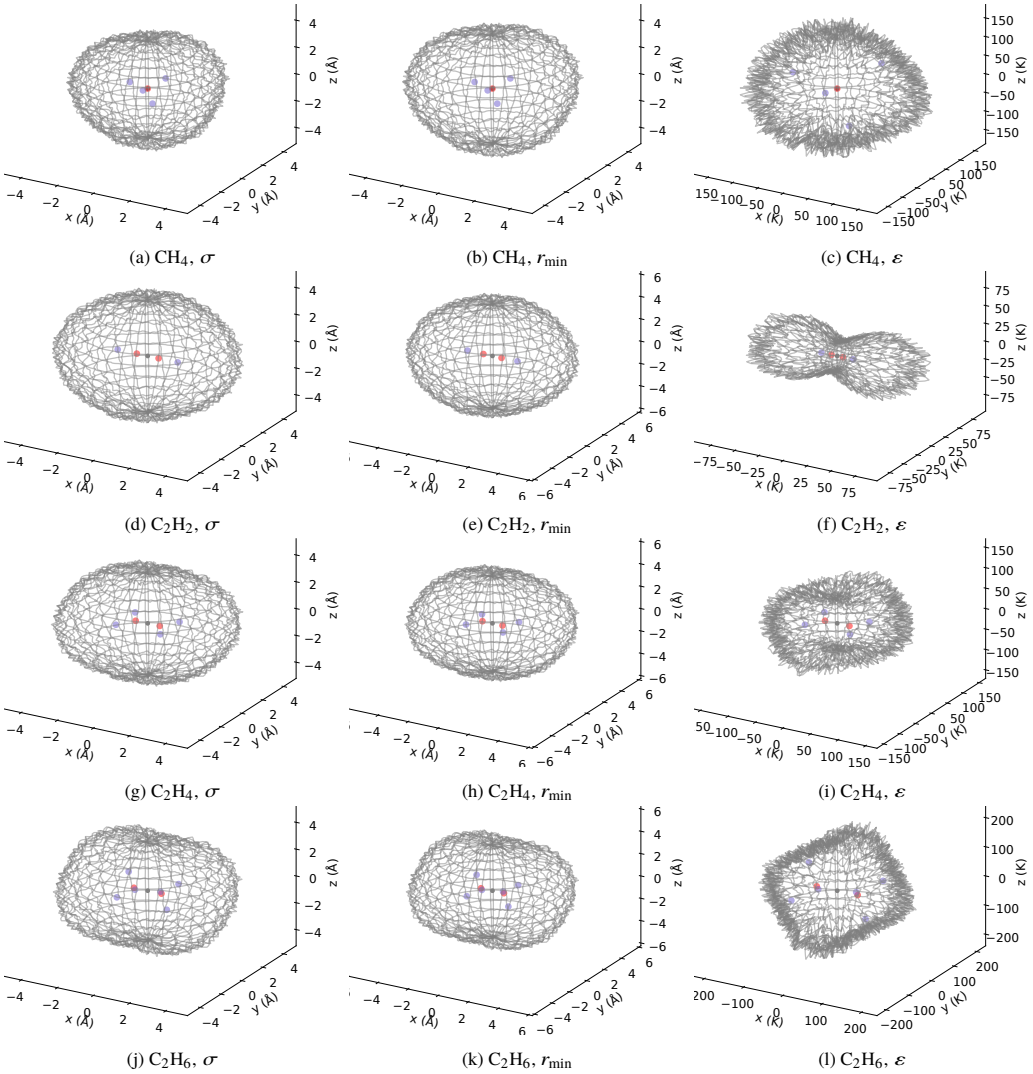

(a) CH_4, σ (b) CH_4, r_{min} (c) CH_4, ε

(d) C_2H_2, σ (e) C_2H_2, r_{min} (f) C_2H_2, ε

(g) C_2H_4, σ (h) C_2H_4, r_{min} (i) C_2H_4, ε

(j) C_2H_6, σ (k) C_2H_6, r_{min} (l) C_2H_6, ε

Figure S-5: Three-dimensional parametric surfaces of the collision diameter σ, well location r_{min}, and well depth ε by the developed iterative search method for a set of target-N_2 pairs. The non-smoothness of related surfaces is due to the self-rotation of the diatomic bath gase during ensemble generation.

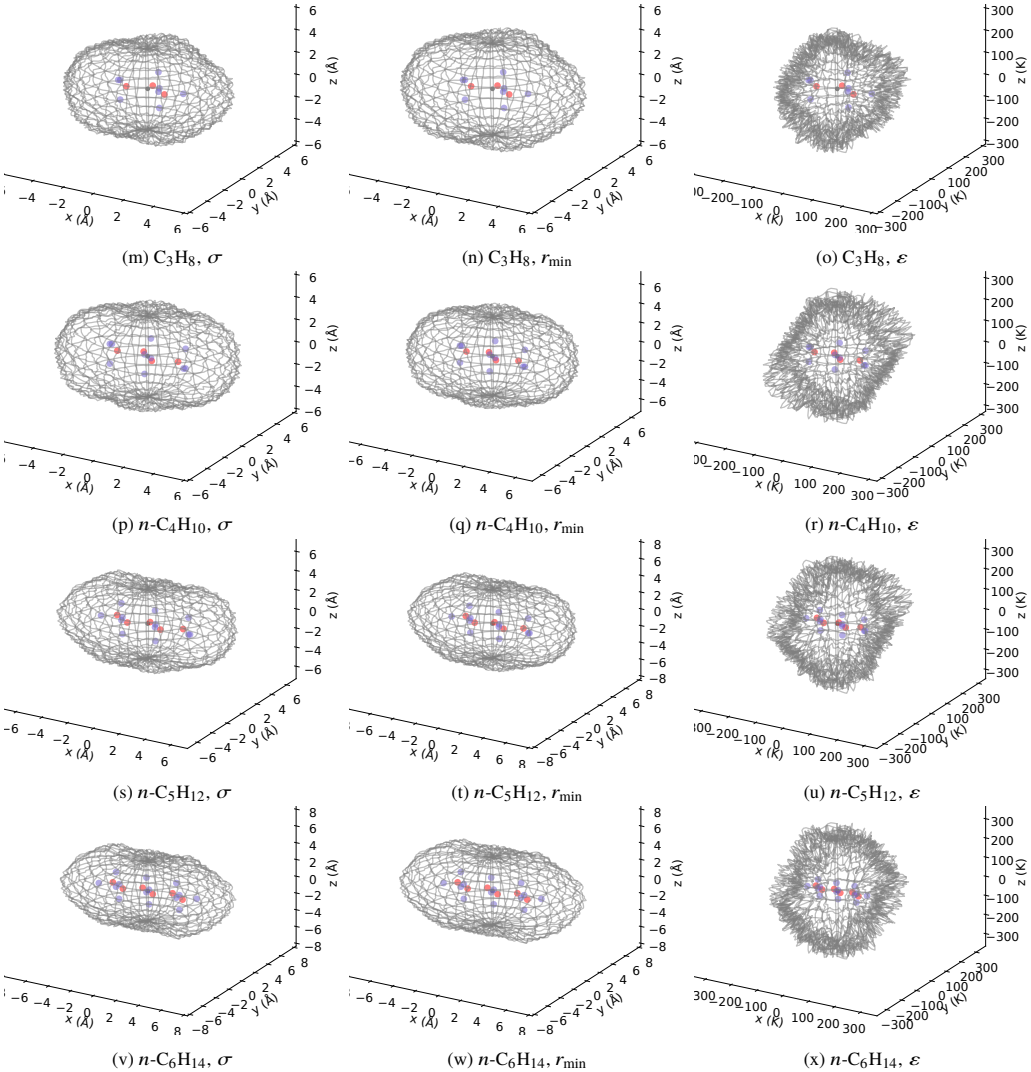

(m) C_3H_8, σ (n) C_3H_8, $r_{\min}$ (o) C_3H_8, ε

(p) n-C_4H_{10}, σ (q) n-C_4H_{10}, $r_{\min}$ (r) n-C_4H_{10}, ε

(s) n-C_5H_{12}, σ (t) n-C_5H_{12}, $r_{\min}$ (u) n-C_5H_{12}, ε

(v) n-C_6H_{14}, σ (w) n-C_6H_{14}, $r_{\min}$ (x) n-C_6H_{14}, ε

Figure S-5: Target-N_2 pairs (continued).

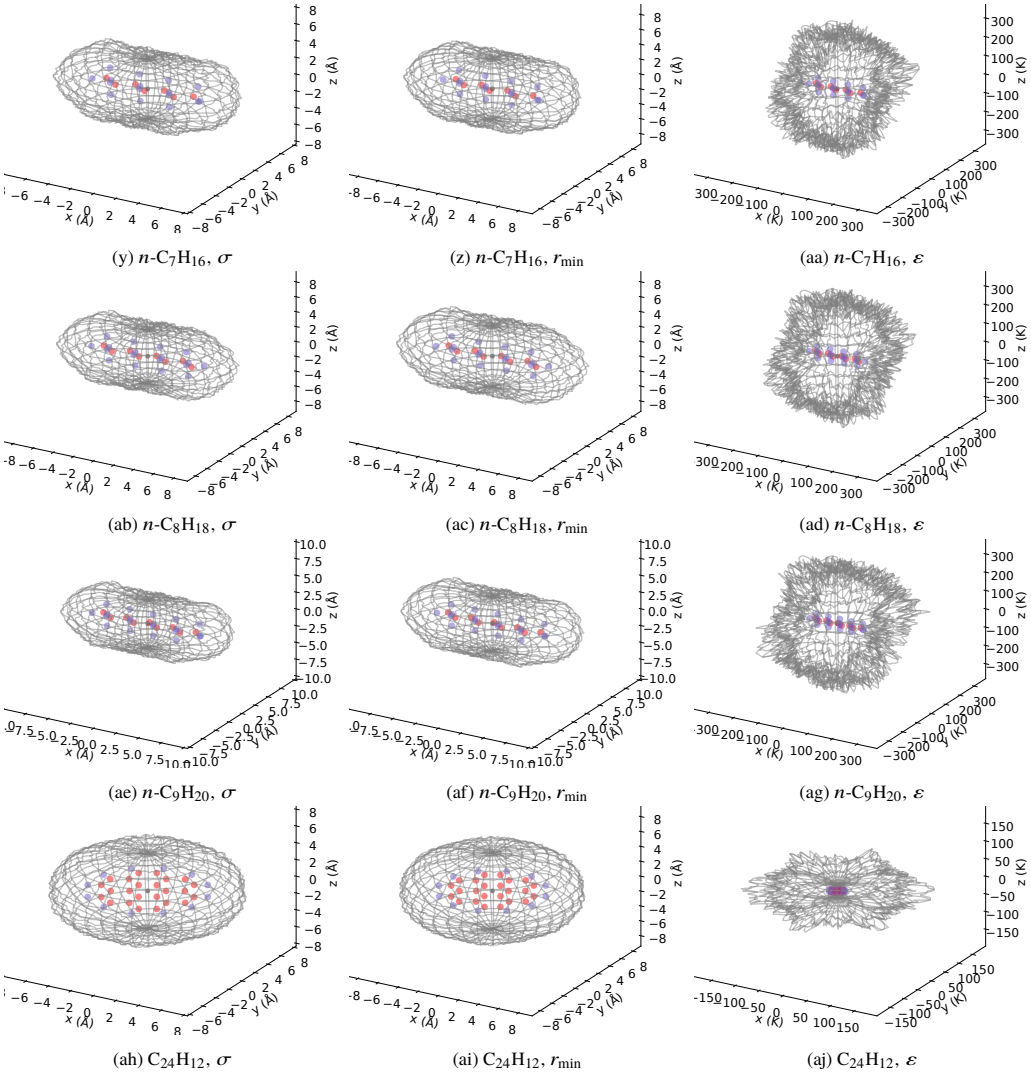

(y) n-C_7H_{16}, σ (z) n-C_7H_{16}, $r_{\min}$ (aa) n-C_7H_{16}, ε

(ab) n-C_8H_{18}, σ (ac) n-C_8H_{18}, $r_{\min}$ (ad) n-C_8H_{18}, ε

(ae) n-C_9H_{20}, σ (af) n-C_9H_{20}, $r_{\min}$ (ag) n-C_9H_{20}, ε

(ah) $C_{24}H_{12}$, σ (ai) $C_{24}H_{12}$, $r_{\min}$ (aj) $C_{24}H_{12}$, ε

Figure S-5: Target-N_2 pairs (continued).

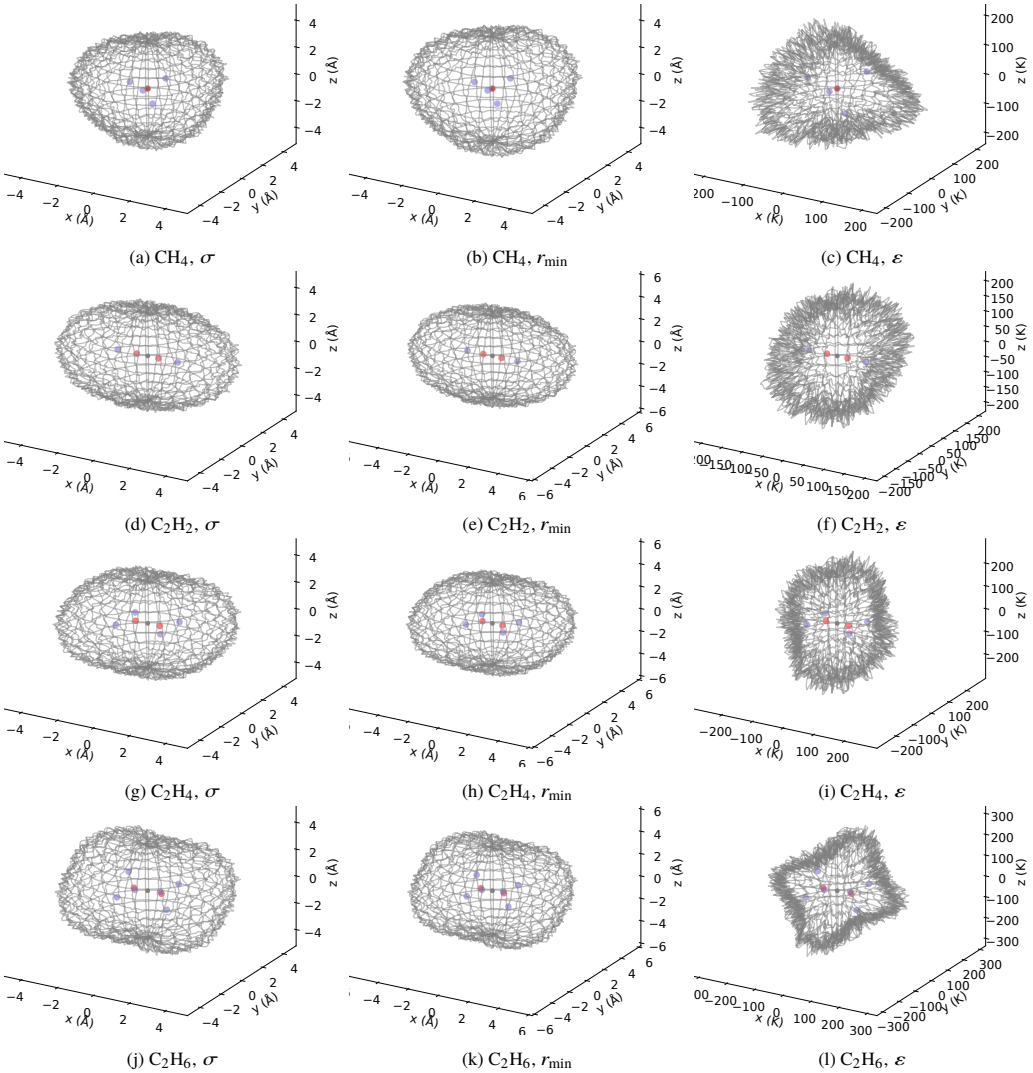

(a) CH_4, σ (b) CH_4, r_{min} (c) CH_4, ε

(d) C_2H_2, σ (e) C_2H_2, r_{min} (f) C_2H_2, ε

(g) C_2H_4, σ (h) C_2H_4, r_{min} (i) C_2H_4, ε

(j) C_2H_6, σ (k) C_2H_6, r_{min} (l) C_2H_6, ε

Figure S-6: Three-dimensional parametric surfaces of the collision diameter σ, well location r_{min}, and well depth ε by the developed iterative search method for a set of target-O_2 pairs. The non-smoothness of related surfaces is due to the self-rotation of the diatomic bath gase during ensemble generation.

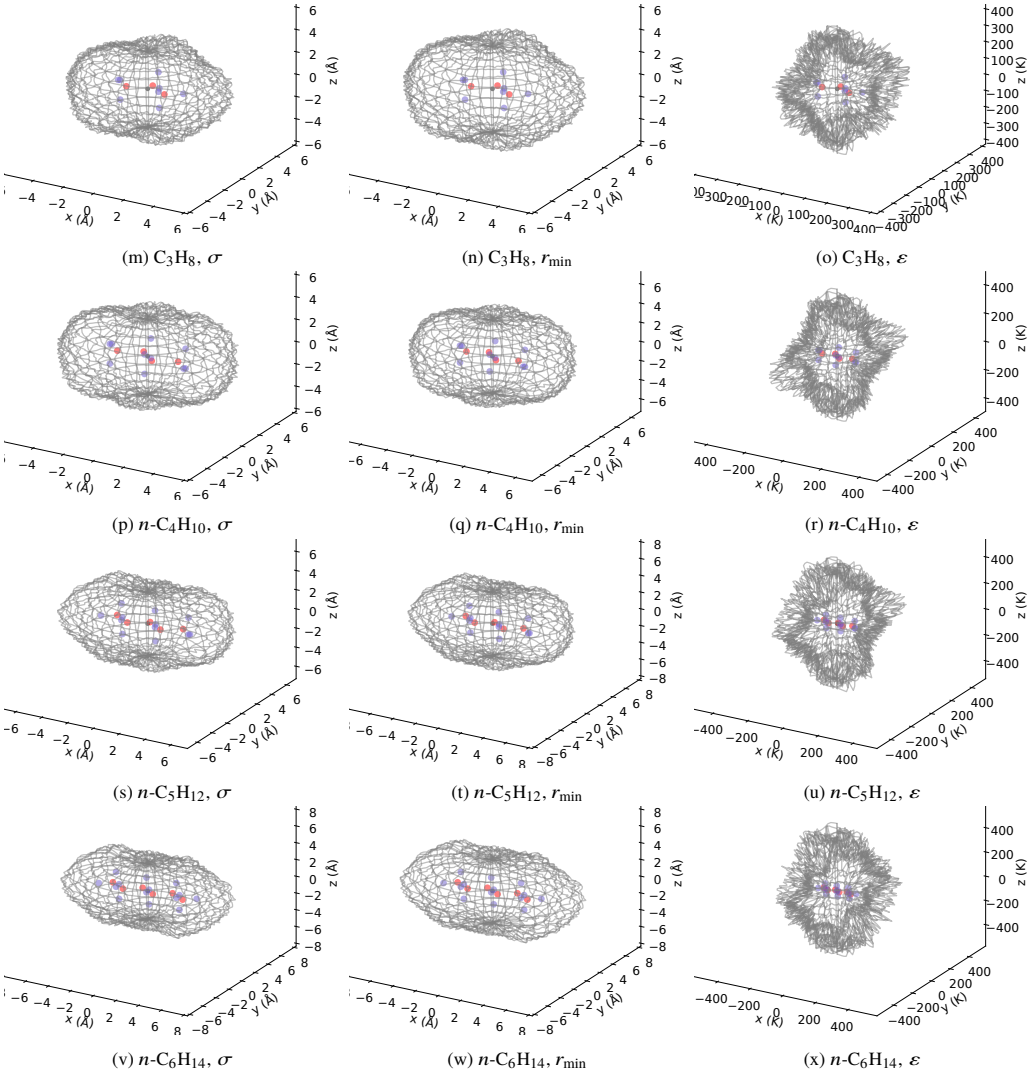

(m) C_3H_8, σ (n) C_3H_8, r_{min} (o) C_3H_8, ε

(p) n-C_4H_{10}, σ (q) n-C_4H_{10}, r_{min} (r) n-C_4H_{10}, ε

(s) n-C_5H_{12}, σ (t) n-C_5H_{12}, r_{min} (u) n-C_5H_{12}, ε

(v) n-C_6H_{14}, σ (w) n-C_6H_{14}, r_{min} (x) n-C_6H_{14}, ε

Figure S-6: Target-O_2 pairs (continued).

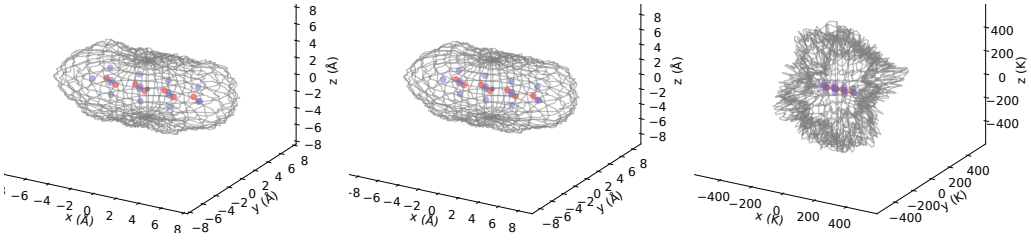

(y) n-C_7H_{16}, σ (z) n-C_7H_{16}, $r_{\min}$ (aa) n-C_7H_{16}, ε

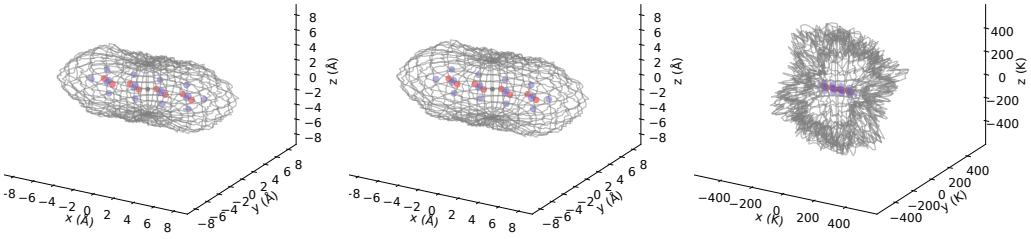

(ab) n-C_8H_{18}, σ (ac) n-C_8H_{18}, $r_{\min}$ (ad) n-C_8H_{18}, ε

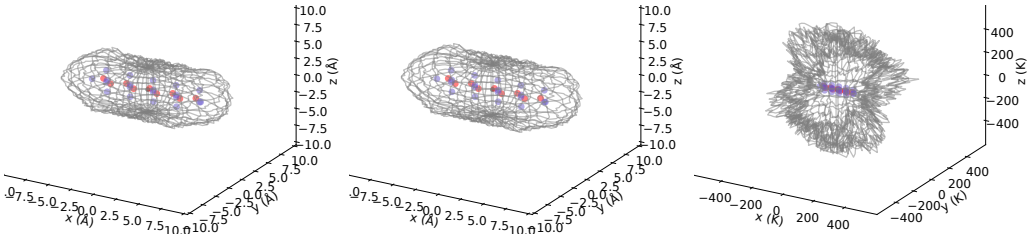

(ae) n-C_9H_{20}, σ (af) n-C_9H_{20}, $r_{\min}$ (ag) n-C_9H_{20}, ε

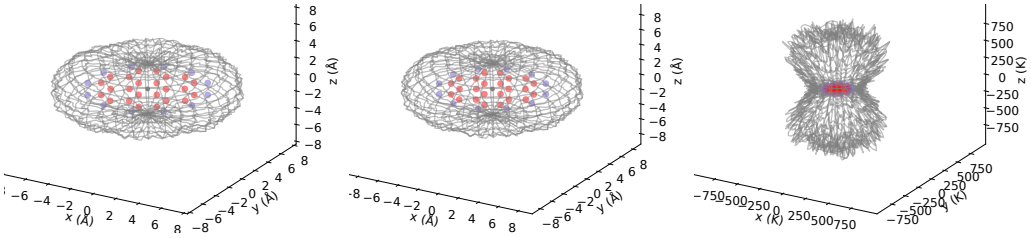

(ah) $C_{24}H_{12}$, σ (ai) $C_{24}H_{12}$, $r_{\min}$ (aj) $C_{24}H_{12}$, ε

Figure S-6: Target-O_2 pairs (continued).